PROCEEDINGS, INDONESIAN PETROLEUM ASSOCIATION
Forty-Sixth Annual Convention & Exhibition, September 2022

CRITICAL POROSITY IN UNDERSTANDING ACOUSTIC POROSITY ANOMALIES. A CASE STUDY IN COMPLEX CARBONATE RESERVOIR IN INDONESIA

Aditya Arie Wijaya*
Sunawar Kunaifi*
Krishna Pratama Laya**
Luqman**
Dimmas Ramadhan**
**Halliburton, ** Medco Energi*

ABSTRACT

The difference between acoustic porosity to total porosity logs has been used to infer the secondary porosity. Apart from gas and/or organic matter, any acoustic porosity with higher reading than total porosity would be considered as an anomaly response. This paper discusses anomalous acoustic porosity in a complex carbonate reservoir, where the acoustic porosity shows higher values than those of the total porosity. The investigation reveals that this anomaly correlates with changes of rock type quality and can be corrected using the critical porosity concept.

The critical porosity links the rock quality to change of the acoustic velocity as a function of critical porosity-bulk modulus for each rock type (Akbar, 2019). Niu et al (2009) proposed the use of shear modulus to determine the critical porosity value. By combining Niu et al (2009) with Akbar (2019) approaches, the critical porosity and critical bulk modulus can be calculated for all rock types.

The result indicates that the critical porosity for each rock type is lower than the proposed value from Akbar (2019). Further analysis from the corrected acoustic porosity suggests that the secondary porosity is low, and this observation is supported by low anisotropy data from dipole sonic. The use of shear as opposed to compressional wave data is better suited in this case study, with a clearer trend in determining the critical porosity.

The case study highlights the importance of the critical porosity concept in understanding anomalies in the acoustic porosity as an effect of rock quality and explaining the preferred method when determining critical porosity values in a gas-bearing complex carbonate reservoir. Further studies may be needed to investigate the critical porosity relationship for poorer rock types in complex carbonate reservoirs.

INTRODUCTION

Carbonate reservoirs are known for their porosity heterogeneity and complexity. Traditionally, the use of sonic logs is considered key to understand the reservoir porosity system, particularly with respect to secondary porosity. The common concept of porosity calculation from sonic travel time (compressional wave) is that the porosity is representing the matrix porosity. Therefore, the difference between sonic porosity and the total porosity from other log measurements, such as density, neutron, density-neutron combination, and/or NMR, would be considered as secondary porosity.

This concept, however, inferred that if sonic porosity is equal to total porosity, then, no secondary porosity exists in the formation. While, if sonic porosity value is lower than that of the total porosity, then the difference represents secondary porosity. This concept has been supported by many publications, most notably the experiment done by Minigalieva et al (2018) using core and well log data on a carbonate reservoir. Their experiment is shown in Figure 1 where the sonic porosity never exceeded 1 p.u. (porosity unit) variance when compared to total porosity (neutron porosity), in rock with vuggy, fractured, or a combination of both.

In the study area (Figure 2), some wells have cores and log data across gas-bearing carbonate reservoirs

* **Haliburton**

with low porosity and low permeability. Integrated petrophysical analyses involving rock typing and permeability modelling have been done in this field. Across all these wells, the calculated sonic porosity has always been higher than total porosity, which is considered to be an anomaly.

In theory, the sonic porosity can only be higher than total porosity when the rock has organic material components, slow velocity rock which is usually attributed to shales, incorrect mud speed in calculation, and/or due to the presence of gas in the reservoir. Upon detailed investigation, none of those conditions can be attributed to the sonic porosity anomaly. However, the anomaly effect appears to be more pronounced in low quality rock (high bulk volume irreducible).

SONIC POROSITY ANOMALY

The sonic porosity is calculated using P-wave data (slowness) and applying the Wyllie equation. The matrix slowness used is 47.8 uspf for limestone, and the oil-based mud slowness of 210 uspf is used. Comparing the total porosity derived from density-neutron cross-plot (PhiNDxp) to the calculated sonic porosity (PhiSon), the sonic porosity indicates much higher values in most of the intervals of the log. The second well, where water-based mud (mud slowness of 189 uspf) was used, also indicates the same porosity anomaly (Figure 3). Therefore, it is believed the mud system is not related to the anomaly.

Investigating the anomaly further, a plot was made from the 1st key well, where the NMR, dipole sonic, and spectral gamma ray are available. Some observations can be drawn from the integrated plot as follows:

Dipole Sonic

The dipole sonic has compressional slowness (DTC) and shear slowness (DTS). It is well known that shear slowness is less affected by gas, and through theoretical value porosity can also be calculated from DTS (DTS_POR) using the same equation as DTC (DTC_POR). Therefore, if the porosity anomaly calculated from DTC is due to the presence of gas, then the porosity from DTS should be less than that calculated from DTC because of gas.

However, it is not the case as can be seen in Figure 4. The DTC_POR and DTS_POR as shown in the Track-7 give the same amount of porosity, despite one being less affected by gas presence. It can be concluded that the anomaly in porosity is not due to the presence of gas.

NMR (Nuclear Magnetic Resonance) and SGR (Spectral Gamma Ray)

The upper part (A) of figure 4a in the same well has slightly higher BVI (Bulk Volume Irreducible) from NMR as shown in Tracks-5 and 8, while having a similar Th-K ratio (Track-9). The BVI or Bulk Volume Irreducible is the amount of bulk volume of water in a rock where it is immovable, typically related to the clay-bound and capillary-bound water. As the BVI gets higher, the permeability would get lower. Similarly, the Th-K is the ratio between Thorium and Potassium in a rock. As this ratio gets higher, the shale volume would increase.

As can be seen in the track-5, the BVI is shifted to higher value across A-section, while the Th-K ratio stays relatively consistent and low throughout A and B sections. The consistent Th-K ratio proves that the higher BVI at the upper part (A) is due to the change in rock quality instead of increased of shale/clay volume.

Furthermore, as the BVI goes higher, the anomaly in sonic porosity (Track-4) gets larger. The conclusion from these two observations is that the acoustic porosity anomaly can be attributed to the change in rock quality (rock type) of the reservoir, which varies throughout the entire well/field. This conclusion is supported by testing several methods explained in the next chapter.

CRITICAL POROSITY

Early Concept

In the simplest terms, the concept of critical porosity aims to account for the non-linearity of sonic velocity and porosity relationship in a rock. In the one hand, the fundamental premise of using sonic to calculate porosity is that the relationship between velocity (1/slowness) and porosity is a linear relationship or fixed against varying rock quality.

In the other hand, Prasad (2003) shows that the velocity of a compressional wave is in relation to permeability (rock quality). Supporting Prasad, Anselmetti and Eberli (1993) as cited by Weger et al (2009) concluded that such variation in velocity at any given porosity is typical in carbonates and relates to the pore structure. Furthermore, Weger et al (2009) also show that the velocity to porosity

relationship can vary between large and small pore systems (Figure 5).

The critical porosity concept was first introduced by Nur et al (1995), where they studied many classes of rocks such as sandstone, dolomites, chalks, and cracked igneous rocks. They proposed a critical porosity value denoted as $\emptyset_C$ as a unique constant, which is typical of a given class of porous material, characterized by its porosity system (after diagenetic process and/or mineralogical composition). The data suggest that the observed values for $\emptyset_C$ can be between 0.005 for cracked granites, and as high as 0.9 for volcanic glasses, as summarized in Figure 6. Without "correction" to sonic porosity, the relationship between velocity and porosity would not be reliable or useful (Nur et al, 1995).

Further Development

Adopting Nur et al. (1995), Akbar (2019) further developed the concept and summarized the approaches, further highlighting the relationship between rock types and velocity. Quantitatively, he suggested an equation to calculate porosity based on acoustic velocity (V_P), bulk density (ρ), critical bulk modulus (B_C), and critical porosity ($\emptyset_C$) as shown in the equation below.

$$\emptyset = \emptyset_C \frac{{V_P}^2\rho - {V_m}^2\rho_m}{B_C - {V_m}^2\rho_m} \quad (1)$$

where V_m and ρ_m are the matrix P-wave velocity and matrix density, respectively. The unit for velocity is in km/s, bulk density is in gm/cc, while bulk modulus is in GPa. The critical bulk modulus can be obtained from the equation below.

$$\frac{1}{B_C} = (1 - \emptyset_C)\frac{1}{B_m} + \emptyset_C \frac{1}{B_f} \quad (2)$$

where B_f is the bulk modulus of the fluid in the pores, and B_m is matrix bulk modulus (quartz = 38 GPa, calcite = 77 GPa).

Akbar (2019) shows a unique value for critical porosity and critical bulk modulus for a given rock type and mineralogy (sandstone versus carbonate), as shown in Figure 7 and listed in Figure 8.

ROCK TYPING

In the studied area, rock typing is key to understand the relationship of velocity and porosity as fully discussed in the previous chapter. Following the work of Akbar (2019), the rock typing based on PGS (Pore Geometry System) is used in the studied area. PGS is a rock type curve by Wibowo and Permadi (2013) that emphasizes the similarity of Kozeny constant as a product of pore shape and tortuosity (Akbar, 2019). The PGS rock typing can be expressed as the following equation.

$$\left(\frac{k}{\emptyset}\right)^{0.5} = a\left(\frac{k}{\emptyset}\right)^{b} \quad (3)$$

where k is the permeability, and $\emptyset$ is porosity. Plotting the above equation in a log-log plot yields a straight line with constant a = 1 and maximum exponent slope of b = 0.5 for perfect rounded pore shape and smooth capillary tube (Akbar, 2019). As the pore system gets more complex, the b value will get lower and vice versa.

A key well in the studied area with complete log and core data is used as reference for the rock typing. The rock typing reveals the presence of eleven rock types (Figure 9), which were later grouped into five dominant rock types as shown in Figure 10, to ease the modelling process.

METHODOLOGY

Critical Porosity and Critical Bulk Modulus Estimation

To correct the sonic porosity using the critical porosity method, one must define the critical porosity and critical bulk modulus value for each rock type. Figure 8 lists the values for critical porosity and bulk modulus from Akbar (2019) covered Rock Type, RT-3 to 10 in carbonate formations. Meanwhile, in the studied area, the rock type span from RT-6 to RT-16. Furthermore, the listed value of critical porosity and critical bulk modulus for carbonate is rather interpretive, as demonstrated in Figure 7, where under the same critical porosity line (coloured dashed line), e.g., RT-4 and RT-5, can overlay under the same critical porosity line.
Instead of using values provided by Akbar (2019), the authors decided to use data from the first key well where core data are available. Using method proposed by Niu et al. (2009) by using shear velocity, V_S instead of compressional velocity, V_P (Akbar, 2019), the critical porosity can be estimated as shown in Figure 11 and the equation below.

$${V_S}^2\rho = a'_S\emptyset_C + b'_S \quad (4)$$

Where, V_S and ρ are shear velocity in km/s and bulk density log in gm/cc, respectively.

The critical porosity then can be calculated when the $V_S{}^2\rho$ is equal to zero, where the trendline intersecting the x-axis (porosity) using the equation below.

$$\emptyset_C = -\frac{b'_S}{a'_S} \quad (5)$$

where the $\emptyset_C$ is the critical porosity.

Applying the same approach to the studied area, Figure 12 shows the result of critical porosity estimation from five different rock types in the studied area. As shown in Figure 12, the x-axis is the NMR porosity value, whereas the y-axis is the $V_S{}^2\rho$. The plotted points in the cross-plot show core points in the logged interval for a given rock type. The NW-SE trendline is drawn based on the distribution of the data and its frequency.

Based on the Niu's method (equations 4 & 5), the critical porosity can be obtained, and the critical bulk modulus can be calculated based on equation 2. The estimated critical porosity and calculated critical bulk modulus based on this method are compared to Akbar (2019) result on each rock type as shown in Figure 13. This new critical porosity and critical bulk modulus will be used in calculating the porosity from sonic logs using equation 1.

RESULT AND DISCUSSIONS

The result is shown in Figure 14 where the comparison is made between sonic porosity before using critical porosity, $\emptyset_C$ (Wyllie method), and after using $\emptyset_C$ applying the V_P method using equation 2 (Akbar, 2019). There are still discrepancies where the sonic porosity is higher than the total porosity (pink shading), but the magnitude is significantly reduced and within the acceptable range (±1 p.u.), particularly across poor quality rocks (RT-4 and RT-5).

What remains as a challenge is the reason why there is difference between the $\emptyset_C$ from Akbar (2019) and the predicted $\emptyset_C$. What can be interpreted from the smaller $\emptyset_C$ is poorer rock quality (low porosity-low permeability) as can be seen in the studied area. It can be also attributed to the fractures as noted by Nur et al. (1995) table in Figure 6. However, upon checking the Stoneley waveform available in this key well, there is no observed reflection that can be attributed to open fractures as shown in Figure 15. There are some depths where Stoneley reflection was observed, but these are related to changing lithology and borehole washout, both are unrelated to fractures.

The borehole image is shown in the Figure 15. However due to the well drilled with OBM (Oil Based Mud), the resolution of this electric borehole image may not be sufficient to delineate fractures.

CONCLUSIONS

From this case study, it can be concluded that the acoustic velocity is not linear in different pore structures and/or geometries (rock types). This effect can result in calculated sonic porosity exceeding the total porosity calculated from other log measurements. This study further supports the previous studies done by several authors that observed variation of velocity at any given porosity is due to variation in pore geometries and/or rock types in the reservoir/logged interval in key and offset wells.

The method suggested by Niu et al. (2009) using shear slowness instead of compressional slowness is better in the studied area for a gas-bearing carbonate reservoir. However, the results indicate that the critical porosity for each rock type is lower than the proposed value from Akbar (2019).

The corrected acoustic porosity (with critical porosity theory) suggests that the secondary porosity is minimum, which is supported by the lack of fracture indication from the Stoneley waveform and borehole image data.

The case study highlights the importance of critical porosity concept in understanding anomalies in the acoustic porosity as an effect of rock quality and explains the recommended method for determining critical porosity values in a gas-bearing complex carbonate reservoir. Further studies may be needed to investigate the critical porosity relationship for poorer rock types in a complex carbonate reservoir.

ACKNOWLEDGEMENTS

The author would like to thank Halliburton and Medco Energi for their full support in publishing this paper.

Special thanks to Anak Agung Gde Iswara A., Ari Subekti, Esterlinda Sinlae, Ricko Rizkiaputra from Medco Energi team, and Banu Andhika, Nuntanich Jittham, and M. S. Iyer from Halliburton Geoscience and Production team.

REFERENCES

Akbar, 2019. New Approaches of Porosity-Permeability Estimations and Quality Factor (Q) Characterization based on Sonic Velocity, Critical Porosity and Rock Typing. SPE Annual Technical Conference and Exhibition, Sep 30 – 2 October, Alberta, Canada. https://doi.org/10.2118/199777-STU

Binhua Niu, et al, 2009. Linear numerical calculation method for obtaining critical point, pore fluid, and framework parameters of gas-bearing media. Applied Geophysics, Vol. 6, No.4, P. 3 19-326.December 2019. DOI:10.1007/s11770-009-0036-8

Laya, K. P., et al, 2021. The Mechanical Stratigraphy of Upper Kutai Basin: Implication to Kerendan Field Development Strategy as Massive Carbonate Tight Gas Reservoir. Proceedings, Indonesian Petroleum Association 40th Annual Convention & Exhibition, September 2021.

Minigalieva, G., et al, 2018. Well Log Analysis for Reservoir Characterization of Famenian Carbonates with Criterion of Texture Heterogeneity. SPE Russian Petroleum Technology Conference, 15-17 October, Moscow, Russia. https://doi.org/10.2118/191677-18RPTC-MS

Nur, A. M., et al., 1995. Critical porosity: The key to relating physical properties to porosity in rocks. In Proceedings of 65th Annual International Meeting of Society of Exploration Geophysicist, vol 878, Tulsa. http://doi.org/10.1190/1.1887540

Prasad, M. 2003. Velocity-permeability relations within hydraulic units. Geophysics 68: 108-117. http://doi.org/10.1190/1.1543198

Weger et al., 2009. Quantification of pore structure and its effect on sonic velocity and permeability in carboantes. AAPG Bulletin, V. 93, No 10, October, PP. 1297-1317. http://doi.org/10.1306/05270909001

Wibowo, A. S., Permadi, P. 2013. A type curve for carbonates rock typing. Presented at the International Petroleum Technology Conference, Beijing, 26-28 March. IPTC-16663-MS. http://doi.org/10.2523/IPTC-16663-MS

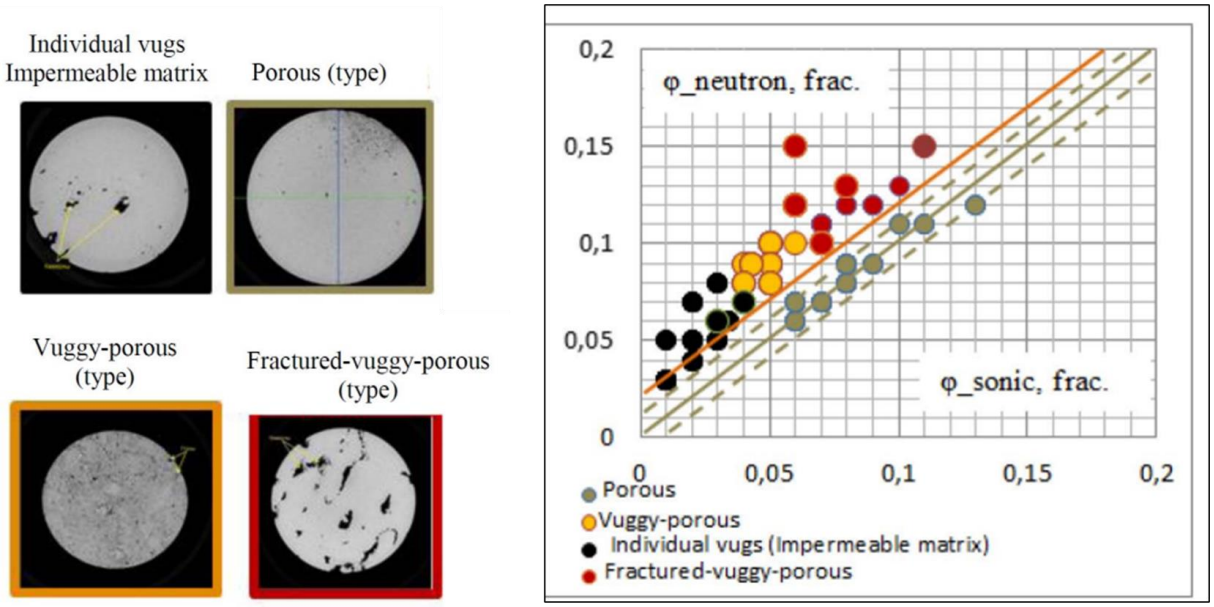

Figure 1 - Cross-plot between porosity from sonic (x-axis) and neutron (y-axis) from four different porosity core types; vuggy-impermeable, porous, vuggy-porous, and fractured-vuggy-porous, Minigalieva et al (2018).

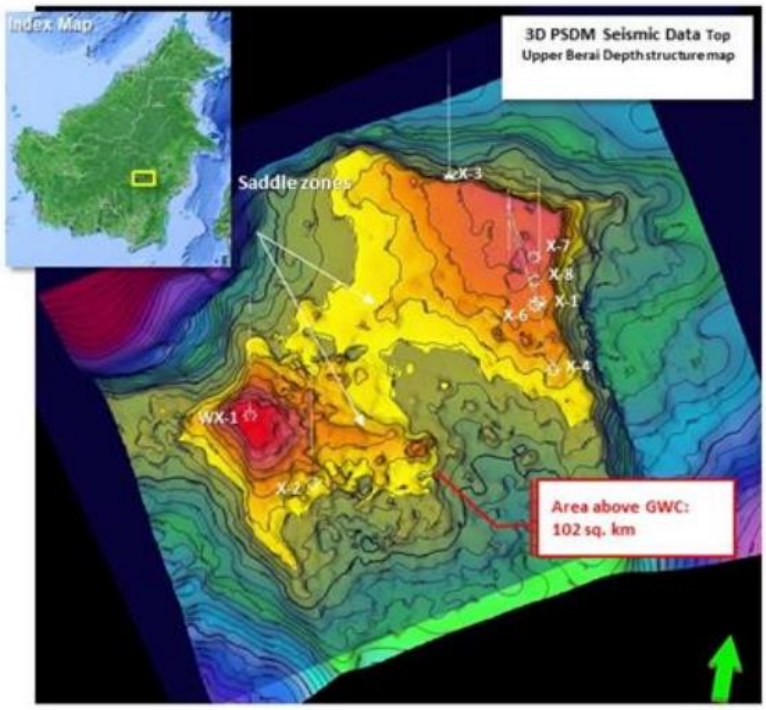

Figure 2 – Location of the studied area, 1st Key Well is WK-1 (Laya, K. P. et al, 2021)

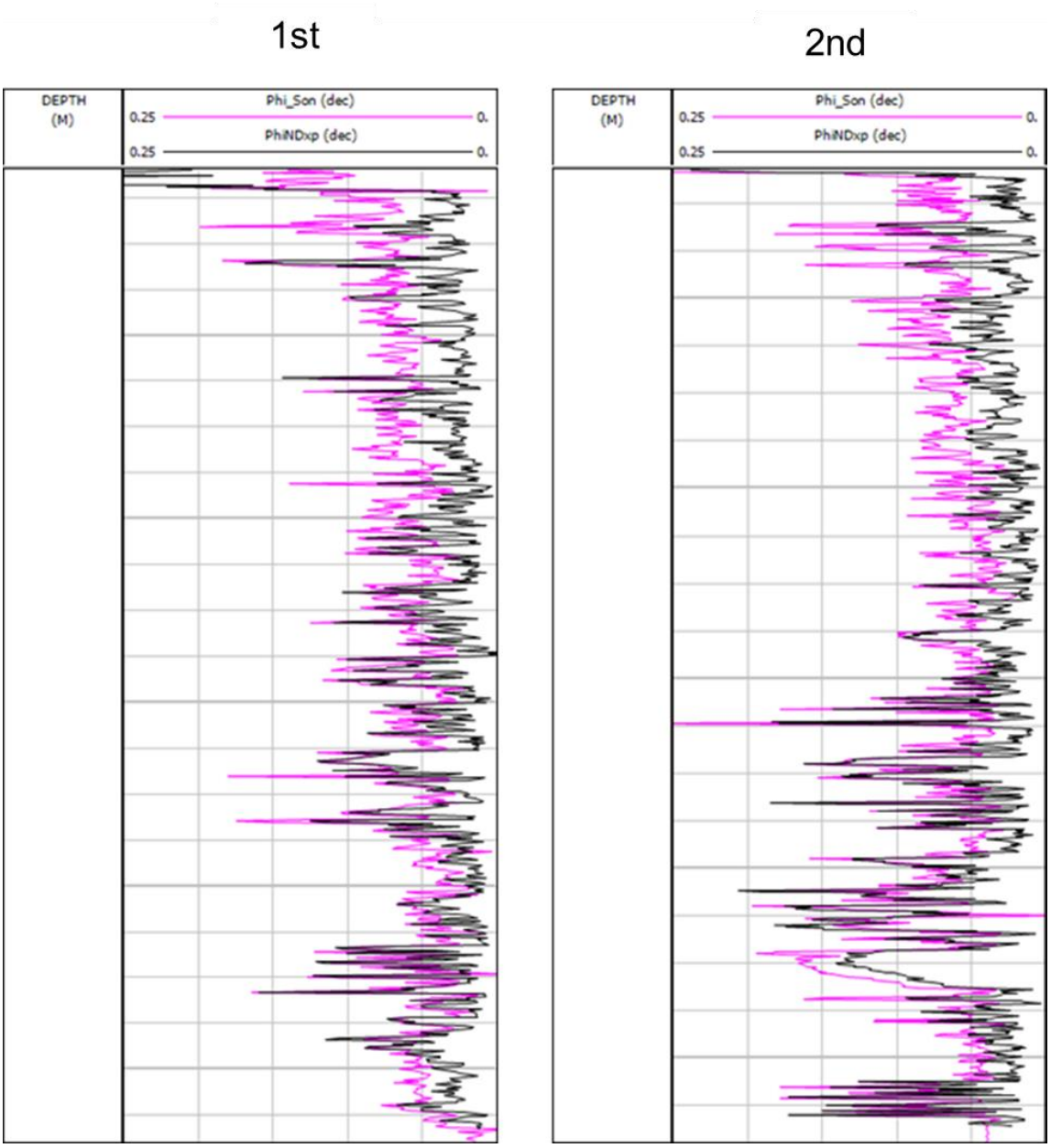

Figure 3 - Two wells with different mud systems (1st OBM, 2nd WBM), with similar anomaly where sonic porosity (PhiSon) is higher than total porosity (PhiNDxp).

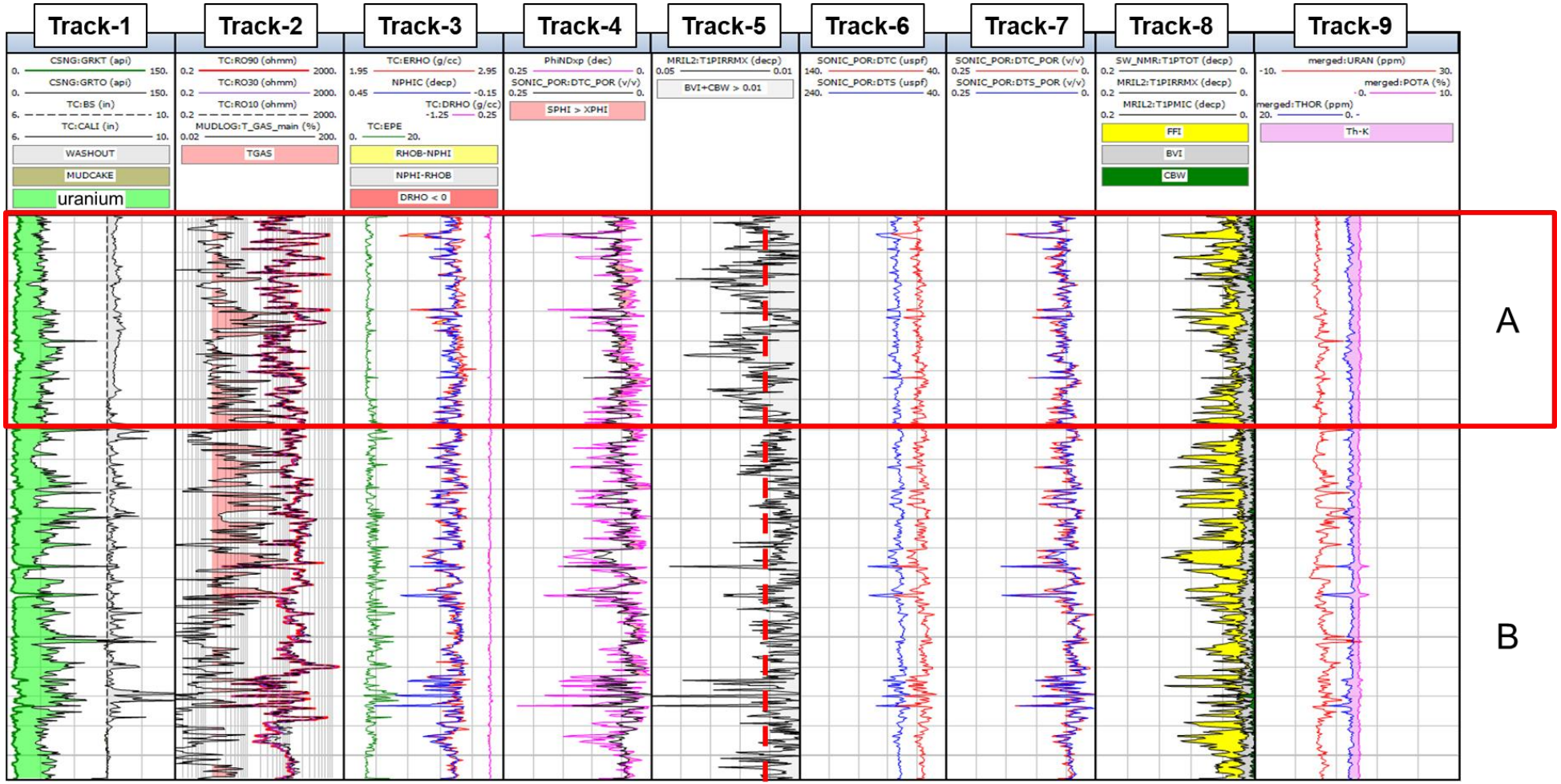

Figure 4 - Integrated plot of 1st key well. Plot shows that the anomaly of sonic porosity is heavily related to the change in BVI (Bulk Volume Irreducible) as shown in track-5 from NMR.

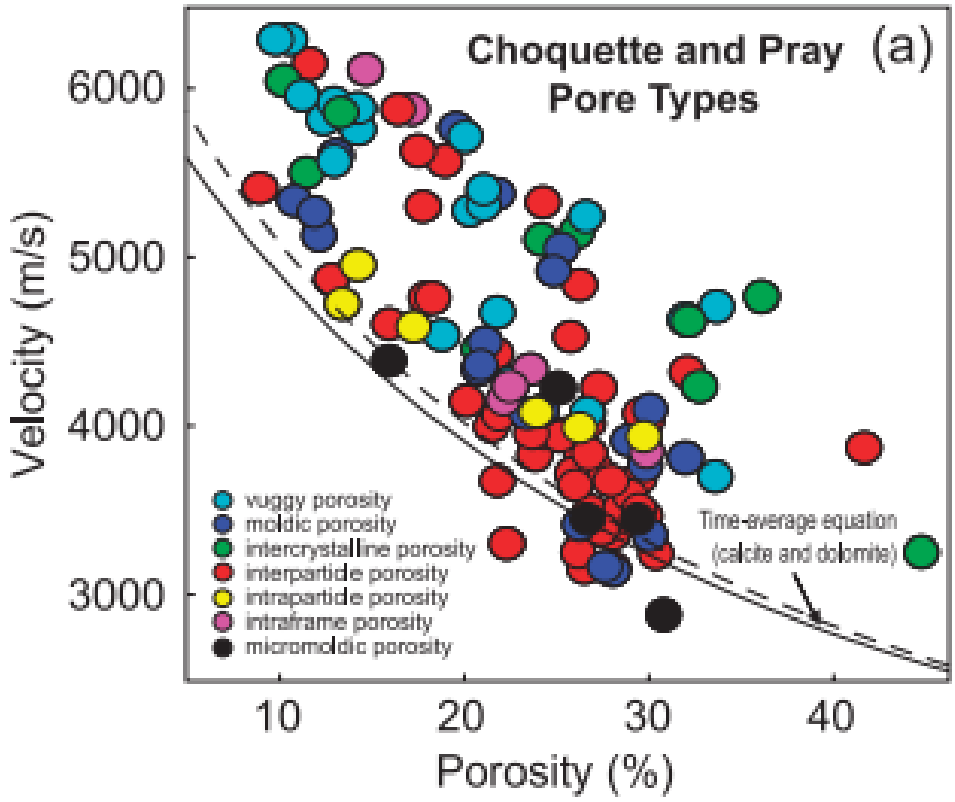

Figure 5 - Cross-plot between velocity and porosity in different pore types (Weger et al, 2009).

ROCK GROUP	CRITICAL POROSITY
Natural Materials	
Cracked Rocks	.005 - .01
Oceanic Basalt	.05 - .15
Limestones	.30 - .35
Dolomites	.30 - .35
Sandstones	.35 - .40
Chalks	.55 - .65
Volcanic Glass	.90
Man-made Materials	
Sintered Glass Beads	.40 - .50
Glass Foam	.90

Figure 6 - Table of different critical porosities for different rock groups of natural and man-made materials (Nur et al, 1995).

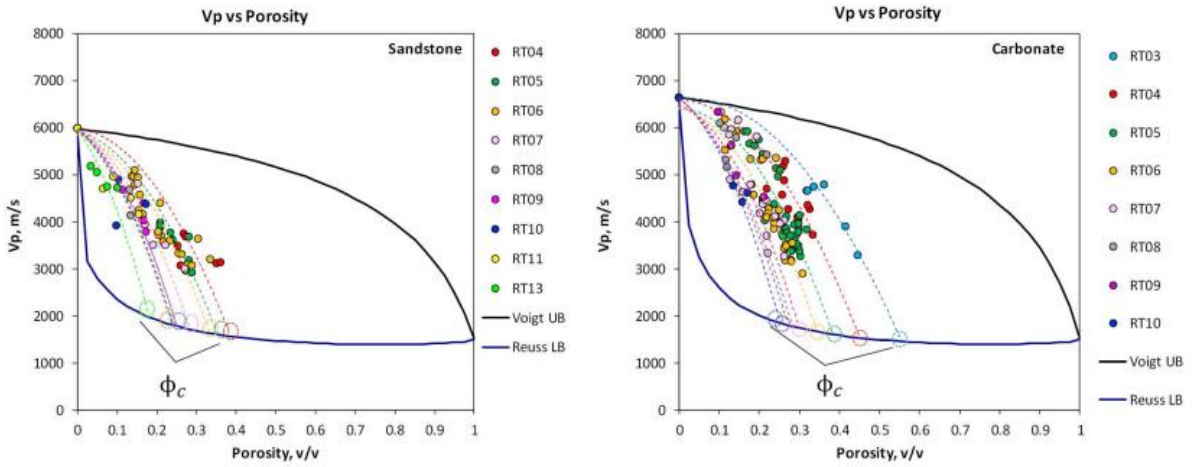

Figure 7 - Cross-plot between velocity and porosity for each rock type in sandstone (left) and carbonate (right). Critical porosity is derived from the trend on each rock type (colored dashed line).

Rock Type	Sandstone		Carbonate	
	ϕ_c	B_c	ϕ_c	B_c
3	-	-	0.55	3.77
4	0.38	5.11	0.45	4.56
5	0.345	5.56	0.38	5.34
6	0.33	5.77	0.34	5.92
7	0.28	6.62	0.3	6.64
8	0.255	7.15	0.28	7.07
9	0.25	7.26	0.27	7.31
10	0.24	7.50	0.25	7.83
11	0.235	7.63	-	-
12	0.18	9.39	-	-
13	0.18	9.39	-	-

Figure 8 - Critical porosity and critical bulk modulus value for each rock type in sandstone and carbonate reservoir (Akbar, 2019).

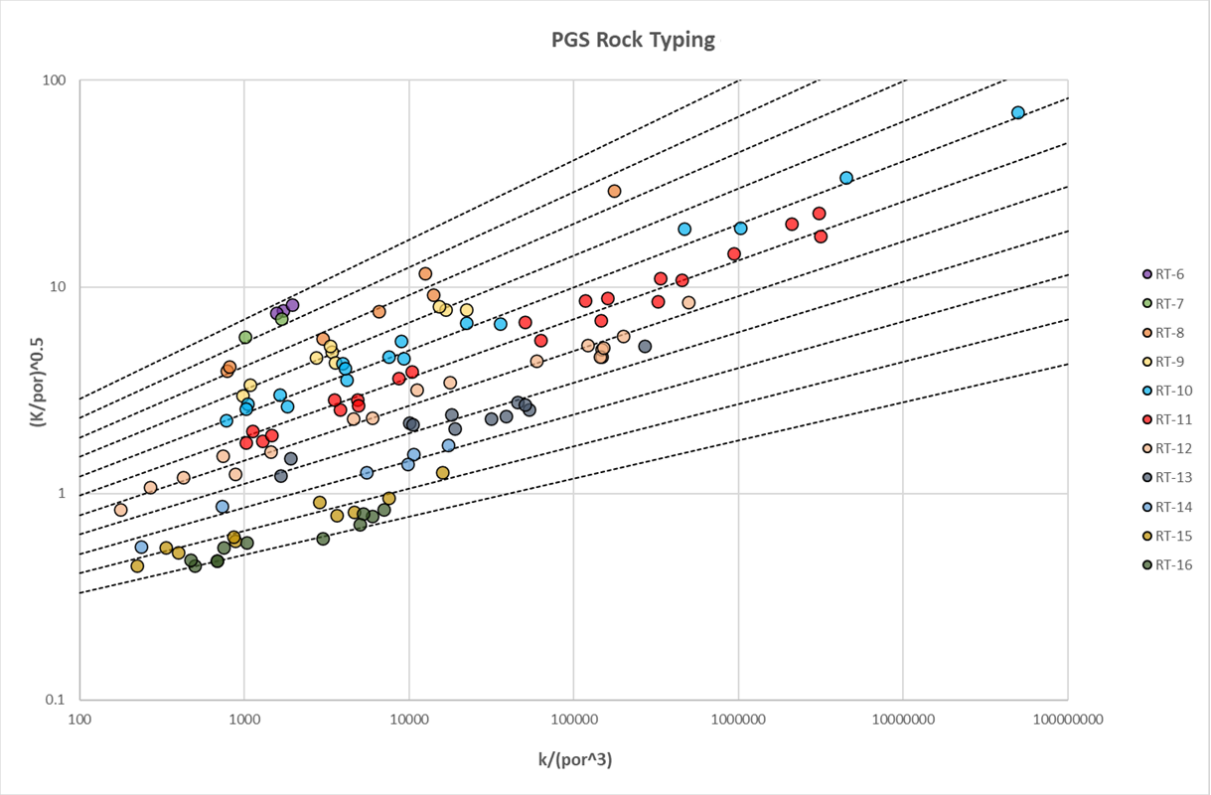

Figure 9 - PGS rock typing in a key well in the studied area.

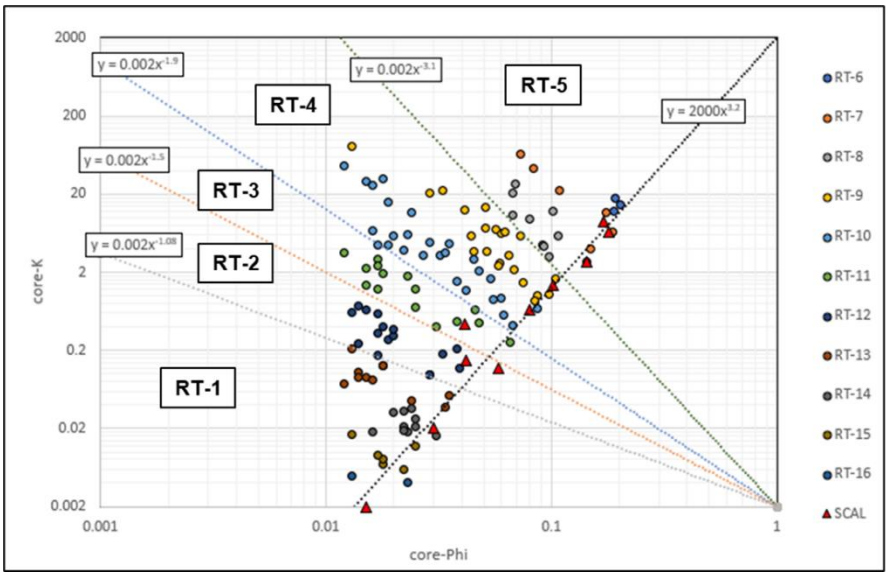

RT-final	RT-ori
	3
	4
	5
1	6
	7
	8
2	9
	10
3	11
4	12
	13
5	14
	15
	16

Figure 10 - A grouped rock type from eleven to five dominant rock types.

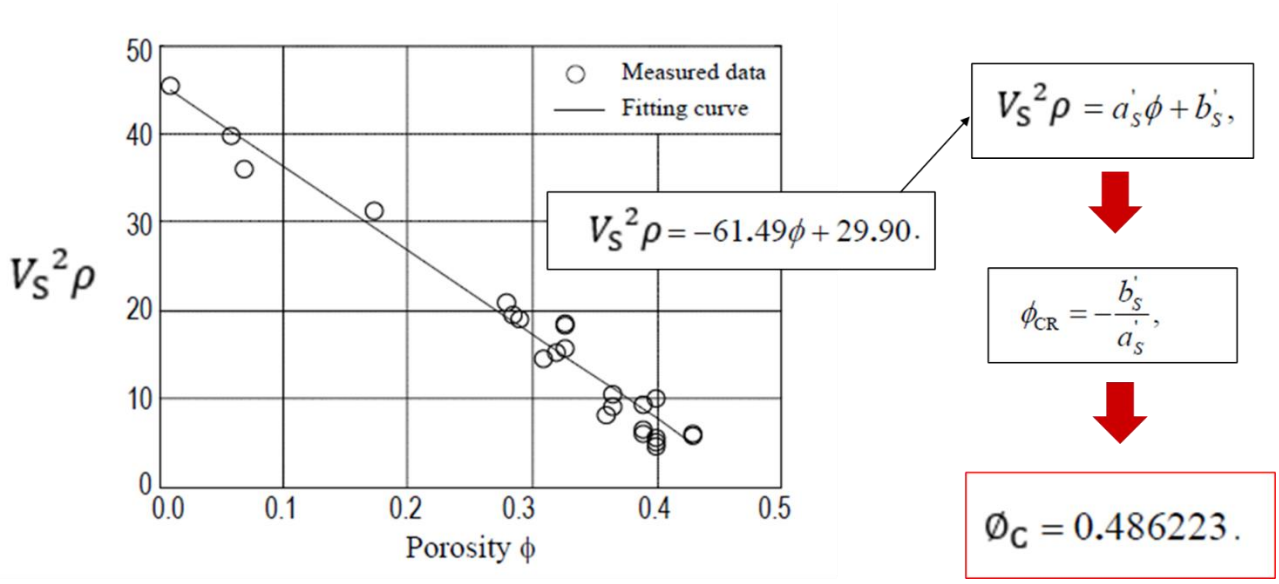

Figure 11 - An example from Niu et al. (2009) where shear velocity can be used to estimate the critical porosity value of a certain rock type.

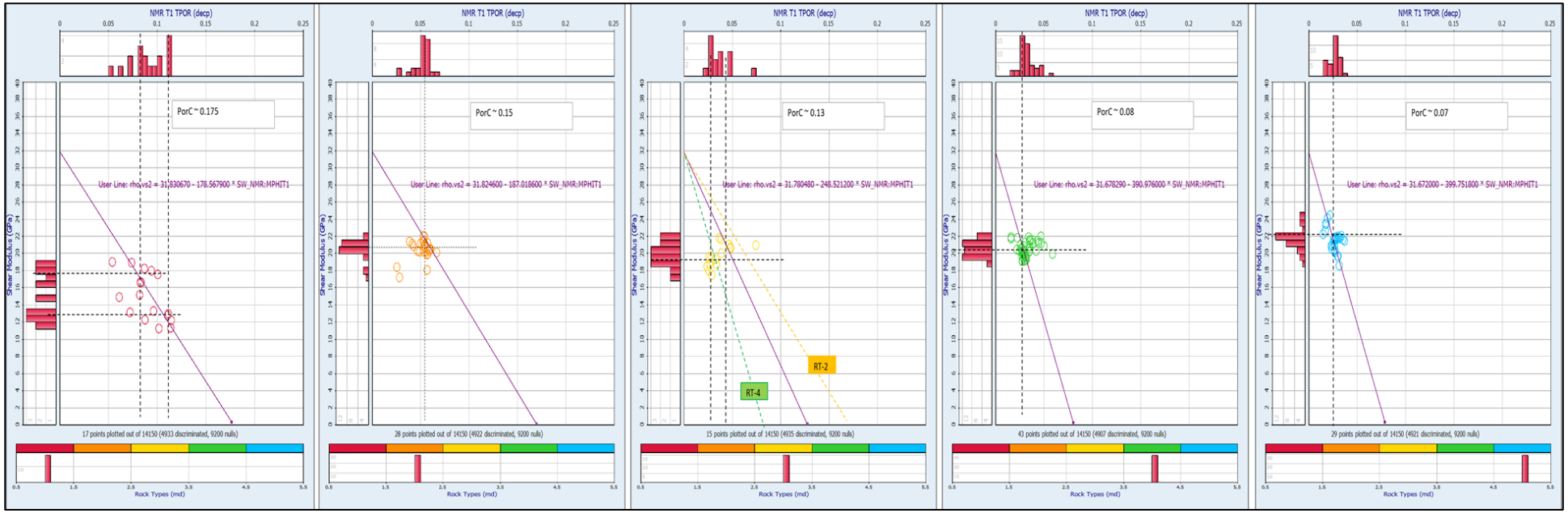

Figure 12 - The estimation of critical porosity from five different rock types using Niu et al (2009) method.

		Akbar, 2019		1st Key Well	
RT-final	RT-ori	$\emptyset_C$	Bc	$\emptyset_C$ _pred	Bc_pred
	3	0.55	3.77		
	4	0.45	4.56		
	5	0.38	5.34		
1	6	0.34	5.92	0.175	8.83
	7	0.3	6.64		
	8	**0.28**	**7.07**		
2	9	0.27	7.31	0.150	9.85
	10	**0.25**	**7.83**		
3	**11**			0.130	10.85
4	**12**			0.080	14.55
	13				
5	14			0.070	15.61
	15				
	16				

Figure 13 - The comparison table between Akbar (2019) method and Niu (2009) method.

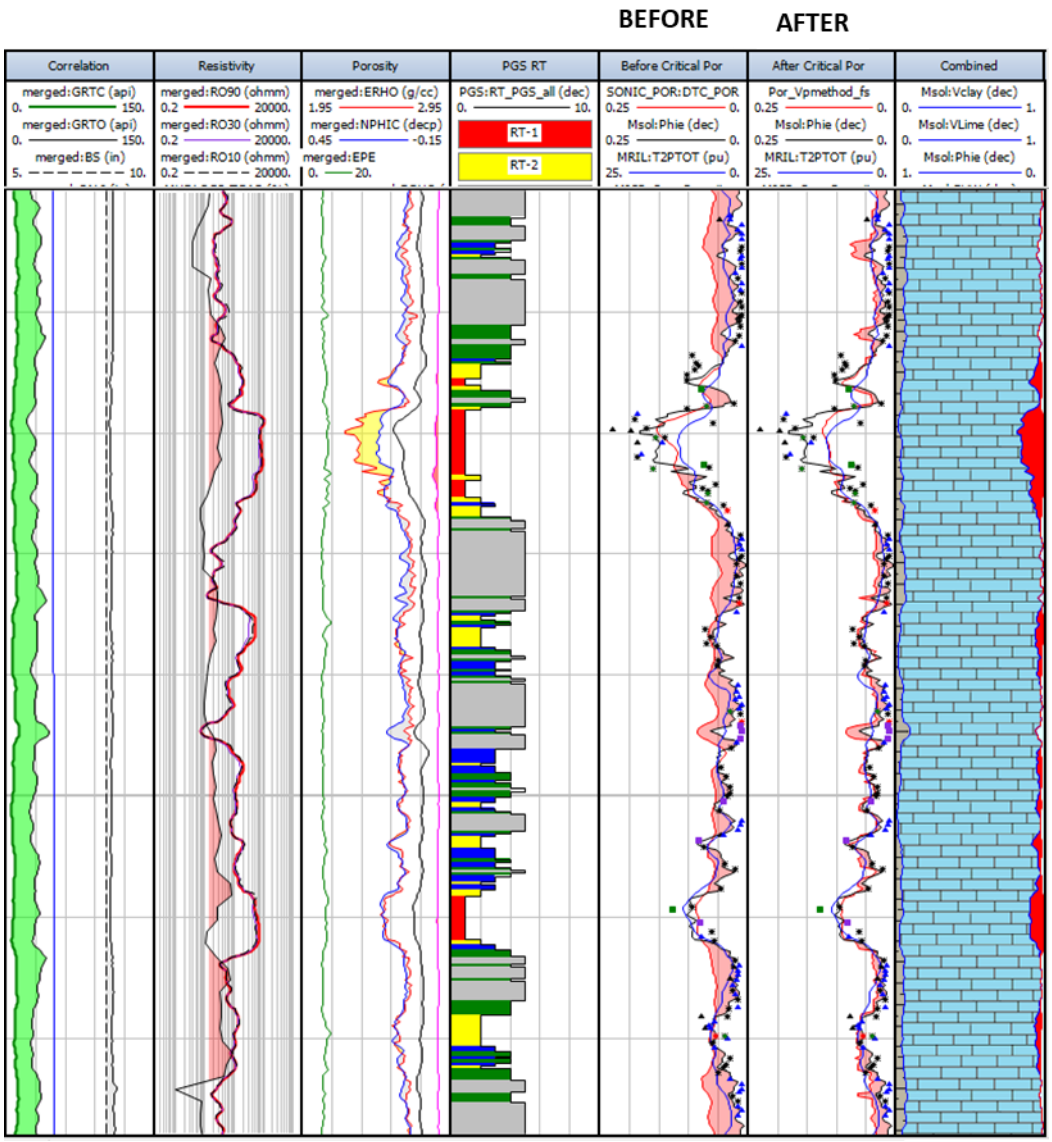

Figure 14 - The comparison (before-after) between sonic porosities calculated using Wyllie method and using Vp method (Akbar, 2019).

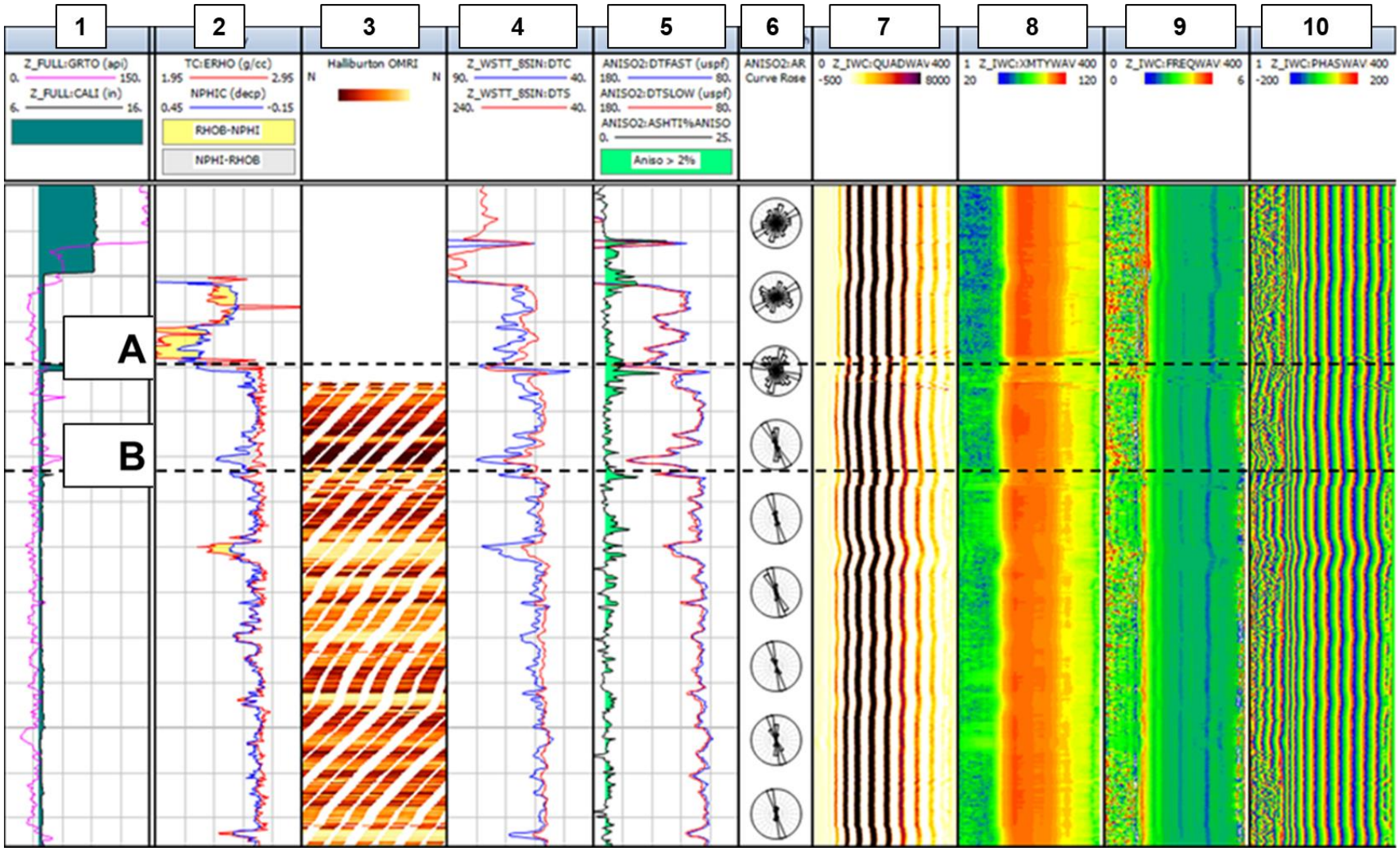

Figure 15 - The borehole image of the well shows some depths where Stoneley reflection was observed, but these are related to changing lithology and borehole washout, both are unrelated to fractures. The resolution of this electric borehole image may not be sufficient to delineate fractures due to oil-based mud.